



Preliminary Study for Cellulolytic Microorganism Isolation from Different Resources, Characterization and Identification: Green Convert of Microcrystalline Cellulose to Nanofibers

Soaad O. Mostafa ^a, Azhar A. Hussain ^a, M. M. Roushdy ^b, Amr M. Shehabeldine ^b, Mohamed S. Hasanin^{c*}

^aBotany Department, Faculty of Women for Arts, Science and Education, Ain Shams University, Cairo, Egypt.

^bBotany and Microbiology Department, Faculty of Science (Boys), Al-Azhar University, 11884, Cairo, Egypt

^cCellulose and Paper Department, National Research Centre, 12622, Dokki, Cairo, Egypt.



Abstract

The presented study deals with the isolation of microorganisms able to produce cellulases which convert microcrystalline cellulose (MCC) to nanocellulose fibers (NCFs) in critical conditions. This conduction, namely, could be defined as the most potent isolate capable of producing such cellulases and has the ability to convert the fibers to nanoscale in situ conditions without any need for chemical or mechanical treatment. The isolates were affirmed that the priorities for the election of cellulolytic isolates are fungi. Three isolates offered good stability in comparison with the other isolates that included bacteria and actinomycetes. *Aspergillus flavus* isolated from the rhizosphere of *Vicia faba* plant and identified morphologically and genetically, and was recorded in gene bank with accession number ON428526. This isolate produced NCFs with a length 96 ± 4.3 nm and a diameter 22 ± 3.8 nm, as well as with high crystallinity and thermal stability. The physiochemical characterizations of the cellulosic fiber produced by the investigated isolate (*Aspergillus flavus*) affirmed that the CNFs had unique features since; they showed excellent stability and homogeneity. This bioconversion applies the produced fibers to biomedical applications such as drug delivery.

Keywords: Cellulose nanofibers; biotechnology; enzymes; *Aspergillus flavus*

1. Introduction

The polymer has been an inherent part of our daily life. Right from ordinary polythene bags to the encasing of tech gadgets, polymers have been used almost everywhere. Such type of polymers/plastic makes up a huge proportion of all the polymers/plastic waste in the world, particularly in the ocean. As useful as it is, the polymer is not the most environmentally friendly material [1]. Our constant use of it has seen huge amounts of it lodged in Arctic sea ice, penetrating into the deepest parts of the ocean and even traveling up the food chain. Hence, there is an urgent need for the development of biodegradable polymeric materials that would not involve the use of the toxic or noxious components in

their manufacture and could be degraded in natural environmental conditions [2].

During recent years significant advances have been made in using and development of biodegradable polymeric materials for life applications. Degradable polymeric biomaterials are preferred because these materials have specific physical, chemical, biological, biomechanical and degradation properties. Wide ranges of natural or synthetic biopolymers capable of undergoing degradation hydrolytically or enzymatically are being investigated for many applications [3].

Biopolymers have a very important and significant role due to their unique characteristics, abundance and biocompatibility [4, 5]. They are biodegradable

*Corresponding author e-mail: sido_sci@yahoo.com ; (Mohamed S. Hasanin).

Receive Date: 26 April 2022, Revise Date: 02 June 2022, Accept Date: 31 July 2022

DOI: 10.21608/EJCHEM.2022.135890.5986

©2022 National Information and Documentation Center (NIDOC)

molecules produced by living organisms such as microorganisms, plants or trees [6, 7]. These materials are monomers that contain (polysaccharides, proteins and nucleic acids). Their biodegradability is a unique feature that takes more attention than fossil polymers [6, 8]. Cellulose is one of the most abundant biopolymers which consists mainly of chains of thousands of glucose monomers bonded together covalently [9]. The nature of cellulosic materials has many types, like woody structures such as seeds, stalks and plants. Such structures are abundant in natural fibers where their cell walls consist of repeated crystalline structures resulting from the aggregation of cellulose chains [1]. Cellulose can be extracted from different biomass sources such as wood, annual plants, crop residues or marine biomass through mechanical and chemical treatments well-known as pulping [10]. Biopolymers together with nanotechnology have already found many applications in various fields including water treatment, biomedical application, energy sector, and food industry [6]. Nanocellulose has a great attention due to its unique properties such as abundance, renewable, high surface area, high strength, tuning its surface properties to reach the desired application and biodegradability [11]. The development of nanocellulose has attracted significant interest in the last few decades due to its desired and potentially useful features. Novel nanocelluloses boost the strongly expanding field of sustainable materials and nanocomposites [12]. Cellulose fiber consists of bundles of single cellulose fibers, which have diameters of 25–30 μm . This single cellulose fiber is made up of bundles of microfibrils, which have diameters of 0.1–1 μm [9]. Nanofibers, which have a diameter in the range of 10–70 nm and lengths of thousands of nanometers, are the constituent of microfibrils [13]. In recent years, there has been only a low awareness in the commercialization of cellulose nanofibers (CNFs) due to its high-cost production process [14, 15]. CNFs are prepared via acid hydrolysis of pure cellulose mostly using inorganic acids in which the treatment of cellulosic materials using acid solutions to break down the polysaccharide into simple sugars is a process known as acid hydrolysis [16]. Hydrolysis of glycosidic bonds is possible in both acid and alkaline media, but much faster hydrolysis occurs at acidic medium. Otherwise, the mechanism involved is the creation of anionic or cationic surface charges on nanofibrils which will thus create repulsive forces in between and facilitate their deconstruction from the matrix [17]. CNFs are prepared via mechanical disintegration using high shear forces and potentially high costs [18, 19]. However, the energy consumption of such mechanical treatment was demonstrated to be extremely high, posing a technological limitation that has slowed the industrial development of CNF production for decades [20]. In

addition, the in situ enzymatic pre-treatment reduces energy consumption in comparison with the pure one. The enzymatic pathway can involve different cellulase enzymes (endoglucanases, exoglucanases and cellobiases) which attack differently the amorphous cellulose structure but always give a prehydrolysis which has a positive effect on further fibrillation [18, 21–23]. Biological hydrolysis can be done using cellulose-digesting enzymes via isolated microbes which have the ability to break down the bonds between the units of cellulose chains and convert them to nanoparticles without using any chemicals or physical force, and then we have nanoparticles with low cost as we neglect the cost of enzymes which are naturally produced by the growth of microbes rapidly [14, 24]. This approach offers a better solution than conventional methods as it produces no toxic residues and can perform under mild conditions, resulting in a less energy-intensive process. Also, the nanocellulose derived through the enzymatic process has more value in applications due to its morphology [25, 26]. Over the past few years, nanocellulose (NC) has been proven to be one of the most prominent green materials of modern times [27]. Therefore, in the present work, the unique microorganisms isolated included bacteria, fungi and actinomycetes were subjected to reduce the cellulose fibers diameter to a nanoscale via in situ methods. The produced fibers were characterized to find out the most potent isolate which has the ability to produce cellulose nanofibers.

the cursor in each paragraph and clicking the required style on the drop-down menus.

2. Materials and methods

Materials

Microcrystalline cellulose (MCC) powder was purchased from Sigma Aldrich, Germany. Dinitrosalicylic acid (DNS) purchased from Sigma Aldrich, Germany. DNS reagent, was prepared by dissolving 10 g of sodium hydroxide, 192 g potassium sodium tartarate (Rochelle salt), 10 g dinitrosalicylic acid (add slowly while stirring), 2 g phenol, and 0.5 g sodium sulphite in 600ml, and then make up to 1 liter. All microbial medium component were purchased from Loba Chem. India. All chemical and reagents used in this work were purchased from Loba Chem. India in analytical grade.

Isolation of cellulose degrading microorganisms

Isolation was made from different environmental sources of soil by using enrichment technique. Isolation of cellulose degrading microorganisms was carried out from the rhizosphere region in the soil. Cellulolytic isolates were selected from all samples by using serial dilutions and spread plate technique. Several sub-samples were taken, homogenized in sterile saline solution 0.85% NaCl (w/v) and serially diluted to suspend the cells and spread plate

technique was done using modified Czapek-Dox's agar medium with replacing the sole carbon source (sucrose) by cellulose as described in previous work with minor modifications [14, 28, 29].

Screening for cellulose degrading isolates

Screening for cellulose degrading isolates was carried out quantitatively and qualitatively. The qualitative assay of cellulase activity was performed on the culture plate using iodine test (solution containing 1% iodine crystals and 2% potassium iodide), which would in 15 min form a bluish-black complex with un-used MCC, demarcating a clear zone around the colonies [30]. Quantitative assay for cellulase activity was carried out using by Dinitrosalicylic Acid (DNS) Method [31, 32].

Morphological identification of fungal isolates

The morphological identification of cellulase producing isolates (fungi) after 4 days of cultivation on Czapek-Dox's agar medium. Photos of the growing fungal isolates were captured using digital camera. The fungal mycelia were examined under light microscope (Olympus) with magnification of 200-800X. The morphological characteristics of the fungal isolates were studied according to the universal keys [33-35]. Morphological identification of most potent isolate was carried out with observing the morphological characteristics (color, texture, and appearance) and microscopic characteristics using light microscope.

Molecular identification of the most potent fungal isolate

The potent fungal isolate was sub-cultured in Czapek-Dox's broth medium and incubated in a shaker incubator at optimum conditions for three days. DNA was extracted from agar cultures using Quick-DNA Fungal Microprep Kit (Zymo research; D6007) following the manufacturer's protocol and supported by Sigma Scientific Services Company (Egypt) [28]. Genetic material was subject to extraction and purification DNA by isopropanol after centrifugation of the previous mixtures as previously described by [36]. PCR was performed by using Maxima Hot Start PCR Master Mix (Thermo; K1051). The primers used were forward ITS1-F (5'-TCCGTAGGTGAACCTGCGG-3') and reverse ITS4-R (5'-TCCTCCGCTTATTGATATGC-3') [37]. The amplified DNA product was separated on 1 % agarose gels in 1X TBE buffer. The identification was achieved by comparing the contiguous 18S rDNA sequence with the 18S rDNA sequence data from the reference and type strains available in public databases GenBank using the BLAST program (National Centre for Biotechnology Information) (<http://www.ncbi.nlm.nih.gov/BLAST/>) [38, 39]. The sequence was aligned using Jukes Cantor Model. The sequence of these strains was recorded in

GenBank and obtained the accession number (ON428526).

Math formulae

Characterizations of produced cellulose nanofibers

Structural changes of samples were studied via Fourier-transform infrared (ATR-FTIR) spectroscopy "Spectrum Two IR Spectrometer - PerkinElmer, Inc., Shelton, USA". Spectral analysis was obtained at 32 scans and 4 cm⁻¹ resolutions in wavenumbers ranging from 4000 to 400 cm⁻¹. The crystalline structure of samples was characterized using X-ray (XRD) [diffractometer](#), Shimadzu 7000, Japan. The crystallinity (Cr.I), the degree of an untreated cellulose and that of treated one with enzyme, could be measured via XRD analysis using the following equation (Eq. (1)) [40, 41]:

$$Cr.I = \left(\frac{I_{002} - I_{am}}{I_{002}} \right) \times 100 \quad (1)$$

Where I₂₀₀, corresponding to the crystalline, is the height of the peak intensity at lattice diffraction 002 and 2θ = 22.4°, while I_{am}, corresponding to the amorphous fraction, is the height of the minimum peak intensity between 002 and the 101 peaks. The I_{am} value appeared almost around 2θ = 18°.

The topography of the prepared samples was analyzed using scanning electron microscopy (SEM, Quanta FEG 250, FEI, Republic of Czech) as well as high-resolution transmission electron microscope (HRTEM) JEOL-JEM-1011, Japan. The images analysis was carried out using ImageJ free software. The [particle size distribution](#) and [zeta potential](#) of the prepared samples were measured, using NicompTM 380 ZLS size analyzer, USA. The [thermal degradation](#) was studied using Perkin Elmer thermogravimetric Analyzer TGA7.

Results and Discussion

Microbial isolation

Isolation and Screening of Cellulose-Degrading isolates

A total of 50 purified microbial strains isolated from different natural reserves in the different region, Out of these strains, 20 fungal isolates showed hydrolyzing zones on agar plates containing CMC-Na after iodine staining (Figure 1). The hydrolyzing zone diameter and colony diameter are listed in Figure 1. As well as preliminary quantitative cellulase assay that confirmed the high productivity of enzyme was corresponding to isolate code (A) (1.2 U/mL) and the moderate productivity was recorded with isolate code (B) (0.6 U/mL) as well as the weak productivity was recorded in isolate (C) (0.3 U/mL).

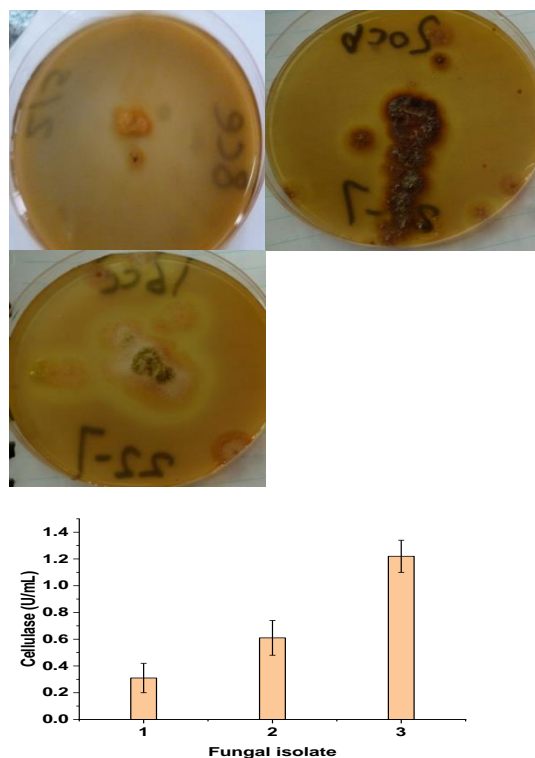


Figure (1): Qualitative cellulase assay (upper) and quantitative cellulase assay (lower) of the fungal isolates.

Morphological identification of the fungal isolates

Result of morphological identification of isolate code (A) showed that fungus that grew on Czapek-Dox's agar medium was as greenish blue spores as well as the light microscope photos confirmed that a yellowish pigment, conidiophores and spores so that Isolate code (A) seems to be of *Penicillium* species. While fungal isolate (B) was isolated from infected *Vicia faba* plant on a PDA medium morphologically was identified as *A. niger*. this strain belonging to the genus *Aspergillus* Section *niger* characteristically present dark-brown to black conidia, with biserial conidiophores, spherical vesicles and hyaline or lightly pigmented hyphae near the apex (Figure 2c). Finally, fungal isolate (C) was isolated from infected *Vicia faba* plant on a PDA medium morphologically was identified as *A. flavus*. Observed colonies on the PDA were 45 mm in diameter at 27 °C after 4 days of growing (Figure 2C). They often display central floccose, white, conidial heads, usually borne uniformly over the whole colony. Characteristically, the colony color is greyish green, yellow green, then becoming greenish in old age. conidia were spherical to sub spheroidal, with relatively thin walls (Figure 2C).

Molecular identification

To validate the morphological identification, molecular identification was performed. The extracted total genomic DNA of the isolated fungal was using to 18S rRNA gene analysis that was amplified using ITS 1 and ITS 4 as

reverse and forward primers into a thermal cycler. The obtained sequencing data were compared with the global recorded database onto national centre for biotechnology information (NCBI) using BLAST program. It confirmed the morphological identification, where the isolated strain code (C) is similar to *A. flavus*, with an identity of 98% (Figure 3). Furthermore, this strain was deposited in GenBank with the accession number ON428526. The phylogenetic tree showed that this strain was much closed to the type strain deposited in the culture collection centre of NCBI as shown in Figure (3).



Figure (2): Morphological identifications: Fungal isolates with 3 days growth on modified Czapek-Dox's agar medium (left) and light microscope examination (right).

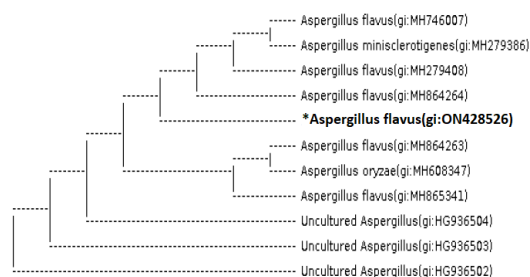


Figure (3): Neighbor-joining phylogenetic tree (Accession no. ON428526).

Characterization of the produced nanofibers

Fourier-transform infrared spectroscopy (FTIR)

FT-IR analysis is used for study the intra and intermolecular structure as well as the functional groups of macromolecules. The FTIR of MCC as well as the three isolates produced treated MCC were illustrated at Figure 4. The OH groups position (stretching mode) was assigned at between 3312 and

3450 cm^{-1} [42] with a maximum value and sharpness for the isolate 3. This may be related to the reducing of cellulose size lead to increase of the surface area and liberated of the new hydroxyl groups [4] at 3445 cm^{-1} (stretching mode) due to the presence of hydrogen-bond of hydroxyl groups. Otherwise, the C-H stretching vibration band was recorded at 2915-2859 cm^{-1} showed significant changes after treated with the fungal isolates in comparison with the pure MCC (2900 cm^{-1}). Moreover, this band was splitted to two small bands in the sample of isolate 3 observed at 2925-2859 cm^{-1} . This may be taken place due to the free and compacted OH groups states made the CH found in two types. In addition, the band of carbohydrate linkage which assigned at 1049 cm^{-1} in the pure MCC was shifted to lower frequency in the cellulose of isolate 1 and 2. However, this band is disappeared to a small band at high frequency poison. These results affirmed that the three isolates produced a modified cellulose with a different size.

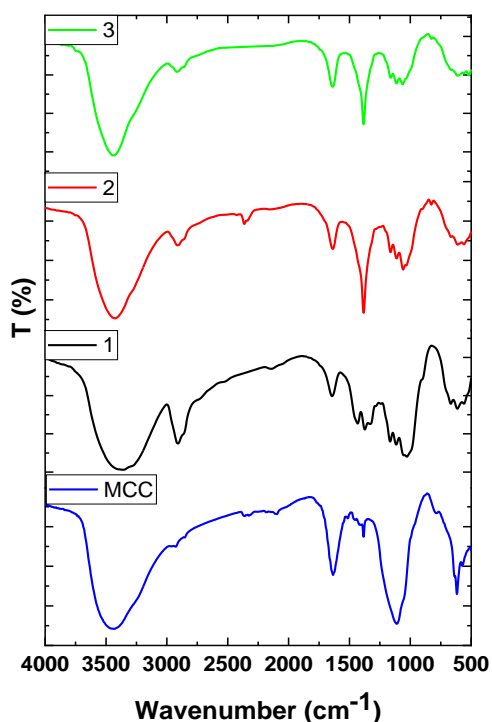


Figure (4): AT-FTIR spectra of MCC and treated samples via fungi isolates.

X-ray diffraction crystallography (XRD)

Figure 5 showed the powder XRD patterns of pure MCC and treated samples. The untreated and treated cellulose showed two characteristic peaks at around $2\theta = 16.1^\circ$ and 22.62° . In the two samples, the XRD peaks correspond to (11 0) and (200) crystal plane, respectively [43-45]. Although, the main characteristic crystallographic peaks of cellulose form all treated cellulose samples via different isolate recognized at the same position with different crystallinity value. Herein, the crystallinity of the

MCC was recorded as 72% as well as the cellulose treated with fungal isolates 1, 2 and 3 were recorded 73, 77 and 80% respectively this may be corresponding to degradation of the amorphous regions of cellulose via fungal cellulolytic enzymes. Worthwhile, the amorphous regions are more reactive to attack by the cellulolytic enzymes that emphasize the increase of the crystallinity parallel with the cellulose enzyme. This result also confirmed the FT-IR analysis.

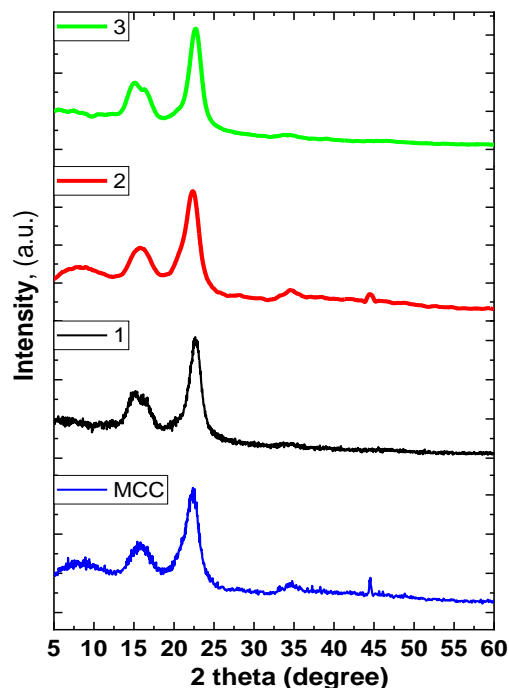


Figure (5): Crystallographic pattern of MCC and treated samples via fungi isolates.

Topography

The topographical studies of the MCC and treated samples with the different fungal isolates were carried out via SEM as well as the fibers sizing were tested using TEM. Figure 6 illustrated the SEM of the tested samples. The MCC (Figure 6-A) surface morphology confirmed a typical cellulosic fibers molecular structure where the fibers compacted together that appears a sheet-like. Otherwise, the fungal treatment via the isolate was affected the surface morphology with a decompaction of the fibers, which showed a more detailed. The samples of rated by isolate 1 (Figure 6-B) and 2 (Figure 6-C) were appeared as fibers with some aggregations. Moreover, the fiber still not of clear shape. On the other hand, the treated cellulose by isolate 3 showed as clear with distinguishable surface morphology (Figure 6-D).

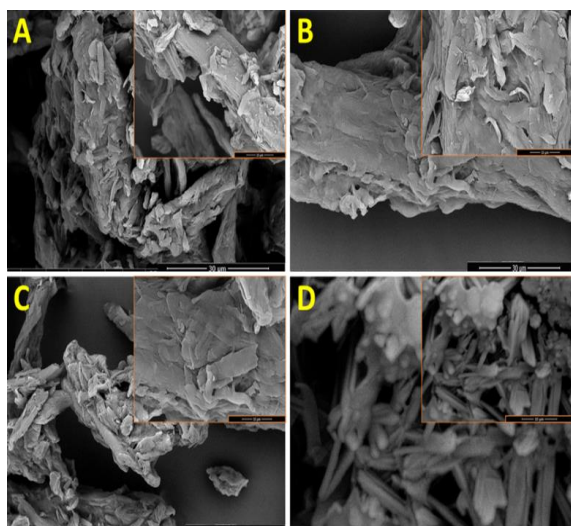


Figure (6): SEM images of MCC (A) and treated samples via fungi isolates 1, 2 and 3 (B, C and D, respectively).

In this context, the TEM images in Figure 7 illustrate the internal structures shape and size distribution of the pure MCC and prepared sample treated with fungal isolates. The pure MCC showed high fiber measurements in size as collapsed fibers. In another way, the cellulosic fibers treated with the fungal isolate represented a high fibrous characteristic material with a needle-like morphology network in the small dimension in comparison with the native one. The sample treated with the isolate 3 (Figure 7-D and F) confirmed the excellent appearance in comparison with the other two isolates, 1 (Figure 7-B) and 2 (Figure 7-C). Whereas isolates 1 and 2 observed an agglomeration in comparison with the sample of isolate 3, which was observed with a low agglomeration in both low and high magnifications. The average diameter and length of the extracted CNFs samples were investigated by analyzing the HRTEM images using open access digital image analysis (Image J) as shown in Figure 7E. From this analysis, the CNFs had 22 ± 3.8 nm for an average diameter and 96 ± 4.3 nm for an average length.

Thermogravimetric analysis (TGA)

The thermal stability of the pure MCC and fungal treated samples were analyzed by TGA as shown in Figure 8. This technique compares the degradation profile of materials which is influenced and representable for the intermolecular structures, various functional groups, the degree of branching, and condensation of cellulosic chains [46]. After absorbed water stage the MCC observed a significant down in weight loss at around 110°C which represented to curing takes place in the cellulose structure. Additionally pure MCC observed two degradation stages at 275 and 315°C . On the other hand, the fungal treated cellulose samples were observed two major peaks at 175°C and 345°C

which may be related to the degradation of crystalline phase of cellulose. Herein, the fungal treated samples were showed the low degradation rate due to the less amorphous content and high condensation [47, 48]. This result is in a nice agreement with the cryptological study and topographical study as well.

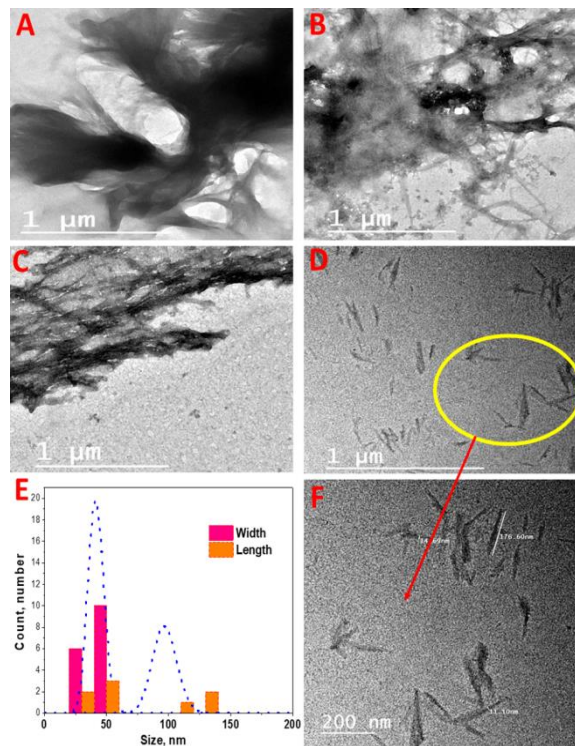
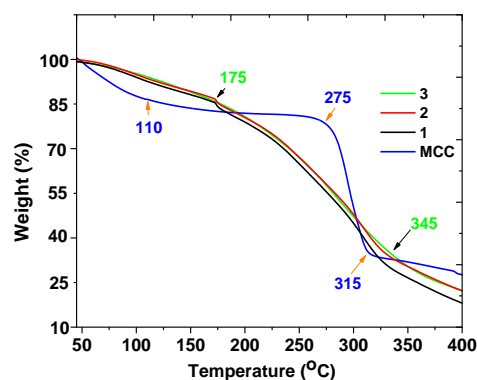


Figure (7): TEM images of MCC (A) and treated samples via fungi isolates 1 (B), 2 (C) and 3 (D, and F) as well as particle size distribution (E).



Figure(8): Thermal analysis of MCC and treated samples via fungal isolates.

Dynamic light scattering (DLS)

The particle size distribution as well as the zeta measurements of MCC and treated sample with fungal isolates were tabulated in Table 1. The particle size distribution of the tested samples was clear where the pure MCC is microcrystals with size around $3.5 \mu\text{m}$.

	zeta potential measurements					Particle size measurements	
	Cell current, mA	Av. Phase shift, rad/sec	Av. Mobility, M.U.	Av. Zeta potential, mV	PDI	Average particle size/ nm	
MCC	1.53	-7.88	-0.31	-3.69	2.952	35151.5	
1	1.1	-12.1	-0.67	-7.33	0.59	802	
2	1.23	-10.32	-0.86	-7.87	0.62	609	
3	0.55	-33.44	-1.42	-20.5	0.22	173	

The treated samples were observed a size less than one micrometer as effect of the fungal treatment and the isolate 3 convert the cellulosic fiber to nano size which recorded as 173 nm and the polydisperse index (PDI) value which consider as the good range between 0-0.3 was recorded for this sample as 0.22 which referred to a good homogeny of particle size distribution. On the other hand, the zeta measurements were confirmed that the sample treated with isolate 3 is exhibited a good stability with average zeta value -20.5 mV which referred to excellent particle stability in the colloidal solutions.

Conclusion

The isolation and identifications of the microorganisms showed that the fungal isolates were of high fitting with the cellulolytic enzymes production than other microbes types. Additionally, the fungal isolates were subjected to the selective parameters included the productivity of Cellulose as well as produced cellulosic fibers specifications. These criteria affirmed that the isolate, namely, *Aspergillus flavus*, is the novel isolate due to the unique properties of its cellulosic nanofibers.

Acknowledgements

The authors present many thanks to the National Research Centre and Al-Azhar University, faculty of Science (Boys) and Faculty of Women for Arts, Science and Education, Ain Shams University for supporting this work, by facilities, as article delivered from MS. Thesis.

Conflict of interest

The authors declare that they have no Conflict of interest

References

- [1] M. Hasanin, A.E.-A. Shaaban, M. Essam, A. Youssef, Compatibility of Polymer/Fiber to Enhance the Wood Plastic Composite Properties and their Applications, Egyptian Journal of Chemistry 64(9) (2021) 5335-5343.
- [2] D. Gnanasekaran, Green Biopolymers and Their Nanocomposites, Springer 2019.
- [3] M.E.S. Hassan, J. Bai, D.-Q. Dou, Biopolymers; definition, classification and applications, Egyptian Journal of Chemistry 62(9) (2019) 1725-1737.
- [4] S. Dacrory, A.H. Hashem, M. Hasanin, Synthesis of cellulose based amino acid functionalized nano-bio-complex: characterization, antifungal activity, molecular docking and hemocompatibility, Environmental Nanotechnology, Monitoring & Management 15 (2021) 100453.
- [5] A. Youssef, A.E.-S. Faze, M.E. Shaaban, Development and Utilization of Chitosan/Carbon Nanocomposite for Heavy Metal Removal from Wastewater, Egyptian Journal of Chemistry (2022).
- [6] S. Mohan, O.S. Oluwafemi, N. Kalarikkal, S. Thomas, S.P. Songca, Biopolymers—application in nanoscience and nanotechnology, Recent advances in biopolymers 1(1) (2016) 47-66.
- [7] A. Shehabeldine, H. El-Hamshary, M. Hasanin, A. El-Faham, M. Al-Sahly, Enhancing the antifungal activity of griseofulvin by incorporation a green biopolymer-based nanocomposite, Polymers 13(4) (2021) 542.
- [8] M. Hasanin, M.A. Elbahnasawy, A.M. Shehabeldine, A.H. Hashem, Ecofriendly preparation of silver nanoparticles-based nanocomposite stabilized by polysaccharides with antibacterial, antifungal and antiviral activities, BioMetals 34(6) (2021) 1313-1328.
- [9] M.S. Hasanin, N. Kassem, M.L. Hassan, Preparation and characterization of microcrystalline cellulose from olive stones, Biomass Conversion and Biorefinery (2021) 1-8.
- [10] A.I. Osman, S. Fawzy, C. Farrell, A.a.H. Al-Muhtaseb, J. Harrison, S. Al-Mawali, D.W. Rooney, Comprehensive thermokinetic modelling and predictions of cellulose decomposition in isothermal, non-isothermal, and stepwise heating modes, Journal of Analytical and Applied Pyrolysis 161 (2022) 105427.
- [11] L. Jasmani, W. Thielemans, Preparation of nanocellulose and its potential application, For Res 7 (2018) 222-228.
- [12] M. Abdelraof, S. Ibrahim, M. Selim, M. Hasanin, Immobilization of L-methionine γ -lyase on different cellulosic materials and its potential application in green-selective synthesis of volatile sulfur compounds, Journal of Environmental Chemical Engineering 8(4) (2020) 103870.

- [13] M.T. Islam, M.M. Alam, A. Patrucco, A. Montarsolo, M. Zoccola, Preparation of Nanocellulose, (2014).
- [14] M.S. Hasanin, A.M. Mostafa, E.A. Mwafy, O.M. Darwesh, Eco-friendly cellulose nano fibers via first reported Egyptian *Humicola fuscoatra* Egyptia X4: Isolation and characterization, Environmental nanotechnology, monitoring & management 10 (2018) 409-418.
- [15] A.M. Shehabeldine, A.H. Hashem, A.I. Hasaballah, Antagonistic effect of gut microbiota of the Egyptian honeybees, *Apis mellifera* L. against the etiological agent of Stonebrood disease, International Journal of Tropical Insect Science 42(2) (2022) 1357-1366.
- [16] S.J. Eichhorn, A. Dufresne, M. Aranguren, N. Marcovich, J. Capadona, S.J. Rowan, C. Weder, W. Thielemans, M. Roman, S. Renneckar, Current international research into cellulose nanofibres and nanocomposites, Journal of materials science 45(1) (2010) 1-33.
- [17] X. Yang, S.K. Biswas, H. Yano, K. Abe, Stiffened nanocomposite hydrogels by using modified cellulose nanofibers via plug flow reactor method, ACS Sustainable Chemistry & Engineering 7(10) (2019) 9092-9096.
- [18] R.S. Ribeiro, B.C. Pohlmann, V. Calado, N. Bojorge, N. Pereira Jr, Production of nanocellulose by enzymatic hydrolysis: Trends and challenges, Engineering in Life Sciences 19(4) (2019) 279-291.
- [19] D.S. Hage, Reference module in chemistry, molecular sciences and chemical engineering, Elsevier Inc., 2013.
- [20] G.K. Gupta, P. Shukla, Lignocellulosic Biomass for the Synthesis of Nanocellulose and Its Eco-Friendly Advanced Applications, Frontiers in Chemistry 8 (2020).
- [21] O. Nechyporchuk, F. Pignon, M.N. Belgacem, Morphological properties of nanofibrillated cellulose produced using wet grinding as an ultimate fibrillation process, Journal of Materials Science 50(2) (2015) 531-541.
- [22] C. Reverdy, N. Belgacem, M.S. Moghaddam, M. Sundin, A. Swerin, J. Bras, One-step superhydrophobic coating using hydrophobized cellulose nanofibrils, Colloids and Surfaces A: Physicochemical and Engineering Aspects 544 (2018) 152-158.
- [23] A.A.F. Elleboudy, M.A. Elagoz, G.N. Simonian, M. Hasanin, Biological factors affecting the durability, usability and chemical composition of paper banknotes in global circulation, Egyptian Journal of Chemistry 64(5) (2021) 2337-2342.
- [24] M. Abdelraof, M.S. Hasanin, H. El-Saied, Ecofriendly green conversion of potato peel wastes to high productivity bacterial cellulose, Carbohydrate polymers 211 (2019) 75-83.
- [25] P. Squinca, S. Bilatto, A.C. Badino, C.S. Farinas, Nanocellulose production in future biorefineries: An integrated approach using tailor-made enzymes, ACS Sustainable Chemistry & Engineering 8(5) (2020) 2277-2286.
- [26] A.M. Shehabeldine, M.A. Elbahnasawy, A.I. Hasaballah, Green phytosynthesis of silver nanoparticles using *Echinochloa stagnina* extract with reference to their antibacterial, cytotoxic, and larvicidal activities, BioNanoScience 11(2) (2021) 526-538.
- [27] T. Djalila, A. Tarchoun, M. Derradji, T. Hamidon, Nanocellulose From Fundamentals to Advanced Applications Enhanced, Front. Chem 8 (2020) 392.
- [28] A.H. Hashem, A.M. Shehabeldine, A.M. Abdelaziz, B.H. Amin, M.H. Sharaf, Antifungal activity of endophytic *Aspergillus terreus* extract against some fungi causing mucormycosis: ultrastructural study, Applied Biochemistry and Biotechnology (2022) 1-15.
- [29] F.R. Nasar, S.A. Nasar, K.A. Abou-Taleb, Tannase and gallic acid production by *Aspergillus niger* SWP33 and *Penicillium griseoforme* T11 using agricultural wastes under submerged and solid-state fermentation and its application, Egyptian Journal of Chemistry 65(9) (2022) 1-5.
- [30] S. Sreedevi, S. Sajith, S. Benjamin, Cellulase producing bacteria from the wood-yards on Kallai river bank, Advances in Microbiology 3(04) (2013) 326.
- [31] M.S. Hasanin, A.H. Hashem, A. El-Sayed, S. Essam, H. El-Saied, Green ecofriendly bio-deinking of mixed office waste paper using various enzymes from *Rhizopus microsporus* AH3: efficiency and characteristics, Cellulose 27(8) (2020) 4443-4453.
- [32] G.L. Miller, Use of dinitrosalicylic acid reagent for determination of reducing sugar, Analytical chemistry 31(3) (1959) 426-428.
- [33] R.A. Samson, E.S. Hoekstra, J.C. Frisvad, Introduction to food-and airborne fungi, Centraalbureau voor Schimmelcultures (CBS)2004.
- [34] K.H. Domsch, W. Gams, T.-H. Anderson, Compendium of soil fungi. Volume 1, Academic Press (London) Ltd.1980.
- [35] J.I. Pitt, The genus *Penicillium* and its teleomorphic states *Eupenicillium* and *Talaromyces*, The genus *Penicillium* and its teleomorphic states *Eupenicillium* and *Talaromyces*. (1979).
- [36] D.A. Levine, F. Bogomolny, C.J. Yee, A. Lash, R.R. Barakat, P.I. Borgen, J. Boyd, Frequent mutation of the PIK3CA gene in ovarian and breast cancers, Clinical cancer research 11(8) (2005) 2875-2878.

- [37] M. Fernandez, A. Figueiras, C. Benito, The use of ISSR and RAPD markers for detecting DNA polymorphism, genotype identification and genetic diversity among barley cultivars with known origin, *Theoretical and Applied Genetics* 104(5) (2002) 845-851.
- [38] S.S. Sobieh, Z.M.H. Kheiralla, A.A. Rushdy, N.A.N. Yakob, In vitro and in vivo genotoxicity and molecular response of silver nanoparticles on different biological model systems, *Caryologia* 69(2) (2016) 147-161.
- [39] K.M. Barakat, S.W. Hassan, O.M. Darwesh, Biosurfactant production by haloalkaliphilic Bacillus strains isolated from Red Sea, Egypt, *The Egyptian Journal of Aquatic Research* 43(3) (2017) 205-211.
- [40] L. Segal, J. Creely, A. Martin Jr, C. Conrad, An empirical method for estimating the degree of crystallinity of native cellulose using the X-ray diffractometer, *Textile Research Journal* 29(10) (1959) 786-794.
- [41] Z.Z. Azrina, M.D.H. Beg, M. Rosli, R. Ramli, N. Junadi, A.M. Alam, Spherical nanocrystalline cellulose (NCC) from oil palm empty fruit bunch pulp via ultrasound assisted hydrolysis, *Carbohydrate polymers* 162 (2017) 115-120.
- [42] M.S. Hasanin, S.A. Al Kiey, Environmentally benign corrosion inhibitors based on cellulose niacin nano-composite for corrosion of copper in sodium chloride solutions, *International Journal of Biological Macromolecules* 161 (2020) 345-354.
- [43] M. El-Sakhawy, M.L. Hassan, Physical and mechanical properties of microcrystalline cellulose prepared from agricultural residues, *Carbohydrate polymers* 67(1) (2007) 1-10.
- [44] W. Xiao, W. Yin, S. Xia, P. Ma, The study of factors affecting the enzymatic hydrolysis of cellulose after ionic liquid pretreatment, *Carbohydrate polymers* 87(3) (2012) 2019-2023.
- [45] A.M. Darwish, W.H. Eisa, A.A. Shabaka, M.H. Talaat, Investigation of factors affecting the synthesis of nano-cadmium sulfide by pulsed laser ablation in liquid environment, *Spectrochimica Acta Part A: Molecular and Biomolecular Spectroscopy* 153 (2016) 315-320.
- [46] W.M. Darwish, A.M. Darwish, E.A. Al-Ashkar, Indium (III) phthalocyanine eka-conjugated polymer as high-performance optical limiter upon nanosecond laser irradiation, *High Performance Polymers* 28(6) (2016) 651-659.
- [47] A. Awad, A.I. Abou-Kandil, I. Elsabbagh, M. Elfass, M. Gaafar, E. Mwafy, Polymer nanocomposites part 1: Structural characterization of zinc oxide nanoparticles synthesized via novel calcination method, *Journal of Thermoplastic Composite Materials* 28(9) (2015) 1343-1358.
- [48] A.I. Abou-Kandil, A. Awad, E. Mwafy, Polymer nanocomposites part 2: Optimization of zinc oxide/high-density polyethylene nanocomposite for ultraviolet radiation shielding, *Journal of Thermoplastic Composite Materials* 28(11) (2015) 1583-1598.